

Research Article

Rain-Induced Bistatic Scattering at 60 GHz

Henry T. van der Zanden,^{1,2} Robert J. Watson,² and Matti H. A. J. Herben¹

¹Department of Electrical Engineering, Eindhoven University of Technology, 5600 MB Eindhoven, The Netherlands

²Department of Electronic and Electrical Engineering, University of Bath, Bath BA2 7AY, UK

Received 27 June 2006; Revised 10 November 2006; Accepted 15 January 2007

Recommended by Peter F. M. Smulders

This paper presents the results of a study into the modeling and prediction of rain-induced bistatic scattering at 60 GHz. The bistatic radar equation together with Mie theory is applied as the basis for calculating the scattering. Together with the attenuation induced by the medium before and after scattering, the received scattered power can be calculated at a given path geometry and known orientations of transmit and receive antennas. The model results are validated by comparison with published measurements. Finally, recommendations are made for future deployments of 60 GHz infrastructure.

Copyright © 2007 Henry T. van der Zanden et al. This is an open access article distributed under the Creative Commons Attribution License, which permits unrestricted use, distribution, and reproduction in any medium, provided the original work is properly cited.

1. INTRODUCTION

Recently there has been considerable interest in the 60 GHz frequency band for short distance fixed point-to-point links (<2.5 km) including the so-called “last-mile” communications. The high oxygen attenuation in this band limits its practical use for longer terrestrial links and for Earth-space communication. The main application therefore is in dense urban environments where a high density of short links might be expected. For point-to-point links, one of the key advantages of the 60 GHz band is the relatively high directivity achievable from a physically small antenna. The narrow beam-widths and low side-lobe levels achievable mean that the signal power outside the narrow main lobe is very low.

This is compounded by the high oxygen attenuation in the 60 GHz frequency band, which results in an even faster decrease of signal power outside the main beam. At 60 GHz the oxygen attenuation is typically between 12 and 15 dB km⁻¹. This high attenuation results in very short frequency-reuse distances making these systems extremely suited for high-link density deployments with minimum interference between the links. However, when rain falls on the link, interference between nearby links can occur due to bistatic scattering.

In 2003, a study was performed by QinetiQ on behalf of Ofcom (the UK Office of Communications) to investigate

bistatic scattering at 60 GHz. This study performed a number of measurements and drafted guidelines to take account for rain scattering in dense networks of 60 GHz point-to-point links. This study concluded that even for modest rainfall rates, <10 mm h⁻¹, bistatic coupling is often evident. The study also highlighted the need for the development of theoretical models such as the one presented here.

The basic theory of bistatic scattering has been well explained in the literature (see [1, 2]). There has been much research work into the effects of bistatic scattering at frequencies other than 60 GHz (see, e.g., [3, 4]). At 94 GHz it has been shown that a first-order approximation of multiple-scattering is sufficient to describe bistatic scattering by rain [4]. The effect of multiple scattering generally increases with increasing frequency. It is expected that the first-order approximation of multiple scattering should be sufficient to describe bistatic scattering of rain at 60 GHz. At both 94 GHz and 60 GHz, the wavelength is comparable to the typical diameters of raindrops.

There are few experimental results on bistatic scattering available at 60 GHz (see [5, 6]). Results of rain-induced bistatic scattering have already been investigated and presented in literature. There is a lot of information available, but no specific models have been produced for the evaluation of rain-induced bistatic scattering at 60 GHz.

2. THEORETICAL BACKGROUND

2.1. Bistatic scattering in rain

Bistatic scattering can be obtained in different ways; by single scattering, first-order multiple scattering, multiple scattering, and by the diffusion approximation. The first-order multiple scattering assumes that the wave interacts only with one particle and suffers from attenuation on its way from transmitter to receiver. The incident waves at the particles are assumed to come directly from the transmitter. The amount of incident power from scattered waves is negligible because of the relative low density of rain drops, even in high rain rates. Gloaguen and Lavergnat [4] have shown that the first-order multiple scattering is sufficient to describe scattering in rain for 94 GHz. Since the wavelengths at 60 GHz and 94 GHz are both of the same order as the raindrop radii, a first-order multiple scattering approximation is expected to be applicable at 60 GHz.

The single particle scattering by rain can broadly be described by the bistatic radar equation [1]:

$$\frac{P_r}{P_t} = \iiint_{V_c} \frac{\lambda^2 G_t G_r A_1 A_2}{(4\pi)^3 R_1^2 R_2^2} \rho \sigma_{\text{bi}} \exp(-\gamma_1 - \gamma_2) dV. \quad (1)$$

P_r is the received power, P_t the transmitter power, V_c the common volume, G_t the gain of the transmit antenna, G_r the gain of the receive antenna, A_1 the attenuation at the path from the transmitter to the common volume, A_2 the attenuation at the path from the common volume to the receiver, R_1 the distance from the transmitter to the common volume, R_2 the distance from the common volume to the receiver, $\rho \sigma_{\text{bi}}$ the scatter cross section of each point in the common volume, and γ_1 and γ_2 the optical distances from the transmitter to dV and from dV to the receiver, respectively.

When narrow-beam antennas are used, (1) can further be simplified. The assumption of modeling the antennas as narrow beams is valid since, in practical point-to-point link deployments at 60 GHz, beamwidths will typically be between 0.5 and 2.5 degrees with the first side-lobe at least 20 dB down from the main lobe. Since the beams are very narrow and the path lengths short, the common volume is relatively small. This permits the additional assumption that the raindrop size distribution in the common volume is constant. The rainfall rate is assumed to be constant which is also likely to be true for a small common volume. Finally, the narrow beam approximation for the antennas allows them to be modeled as constant-gain cones. This last assumption gives rise to slight overestimation of the received power, but yields a straightforward analytical solution to V_c (see [1]):

$$V_c = \frac{\pi \sqrt{\pi}}{8(\ln 2)^{3/2}} \frac{R_1^2 R_2^2 \theta_1 \theta_2 \phi_1 \phi_2}{[R_1^2 \phi_1^2 + R_2^2 \phi_2^2]^{1/2}} \frac{1}{\sin \theta_s}, \quad (2)$$

where θ_1 and Φ_1 are the half-power beamwidths of the transmitter and θ_2 and Φ_2 are the half-power beamwidths of the receiver. $\rho \sigma_{\text{bi}}$ can then be replaced with $\rho \langle \sigma_{\text{bi}} \rangle$, the total cross-section per unit volume and the integral over V_c becomes a

straightforward product:

$$\frac{P_r}{P_t} = \frac{\lambda^2 G_t G_r A_1 A_2}{(4\pi)^3 R_1^2 R_2^2} \rho \langle \sigma_{\text{bi}} \rangle \exp(-\gamma_1 - \gamma_2) V_c. \quad (3)$$

$\rho \langle \sigma_{\text{bi}} \rangle$ is dependent on the raindrop size distribution and the scattering cross section. The relationship between them is

$$\rho \langle \sigma_{\text{bi}} \rangle = \int_0^\infty n(D, \bar{r}) \sigma_{\text{bi}}(D) dD, \quad (4)$$

where σ_{bi} is the bistatic scattering cross section and $n(D, \bar{r}) dD$ is the number of drops per unit volume located at \bar{r} having a range of sizes between D and $D + dD$.

To calculate $\rho \langle \sigma_{\text{bi}} \rangle$ for raindrops and signals with a frequency between 58 and 66 GHz, Mie theory is a good option. The use of Mie theory requires the approximation that raindrops are spheres (see [7]). While raindrops are only spherical for small drop radii, the uncertainty in the raindrop size distribution is likely to outweigh the difference between modeling the raindrops as spheroids, which would be more accurate.

2.2. Mie theory

Mie theory describes an exact solution to the scattering properties of an isotropic, homogeneous sphere having radius a , with an incident plane electromagnetic wave [2].

In contrast to the geometrical optics approximation (requiring $\lambda \ll D$) and the Rayleigh approximation (requiring $\lambda \gg D$), Mie theory can be used for all possible ratios of diameter to wavelength. For raindrops and frequencies between 58 and 66 GHz, the wavelength and the diameter are of similar order.

To calculate the scattering cross sections of raindrops and the extinction cross sections of raindrops with Mie theory, the amplitude functions defined in classical Mie theory are used [8]:

$$S_1(\theta_s) = \sum_{n=1}^{\infty} \frac{2n+1}{n(n+1)} (a_n \pi_n(\cos \theta_s) + b_n \tau_n(\cos \theta_s)), \quad (5)$$

$$S_2(\theta_s) = \sum_{n=1}^{\infty} \frac{2n+1}{n(n+1)} (a_n \tau_n(\cos \theta_s) + b_n \pi_n(\cos \theta_s)).$$

The functions a_n and b_n are terms involving spherical Bessel functions, the complex refractive index, and the functions τ_n and π_n which are terms involving the Legendre polynomials.

The extinction cross sections for perpendicular (\perp) and parallel (\parallel) incident waves are:

$$\sigma_{\text{ext}\perp}(\theta_s) = \frac{2\pi a^2}{x^2} \Re \{S_1(\theta_s)\}, \quad (6)$$

$$\sigma_{\text{ext}\parallel}(\theta_s) = \frac{2\pi a^2}{x^2} \Re \{S_2(\theta_s)\},$$

where the size parameter $x = ka$, in which the wavenumber $k = 2\pi/\lambda$.

A raindrop can be seen as a particle illuminated with incident power from the transmitter which it then re-radiates

like a directive antenna. The gain functions for a raindrop with a perpendicular and parallel polarized wave are [3]

$$\begin{aligned} G_1 &= \frac{4i_1}{x^2}, \\ G_2 &= \frac{4i_2}{x^2} \end{aligned} \quad (7)$$

with $i_1 = |S_1(\theta_s)|^2$ and $i_2 = |S_2(\theta_s)|^2$. The antenna gain function is defined by

$$G = \frac{4\pi A_{\text{eff}}}{\lambda^2}. \quad (8)$$

By combining those gain functions of the raindrop and the antenna gain function, the effective aperture of a raindrop can be calculated. This effective aperture is the scattering cross section. This analysis yields in the following functions for the scattering cross section for perpendicular and parallel incident waves:

$$\begin{aligned} \sigma_{\text{sca}\perp}(\theta_s) &= \frac{\lambda^2}{4\pi} \frac{4i_1}{x^2} = \frac{\lambda^2}{\pi x^2} |S_1(\theta_s)|^2, \\ \sigma_{\text{sca}\parallel}(\theta_s) &= \frac{\lambda^2}{4\pi} \frac{4i_2}{x^2} = \frac{\lambda^2}{\pi x^2} |S_2(\theta_s)|^2. \end{aligned} \quad (9)$$

2.3. Link geometry

The geometry of the link (altitude and elevation of the antennas) is an important factor in the scattering calculation. The geometry has to be taken into account in order to accurately calculate the line-of-sight distances and R_1 and R_2 . A difference in altitude between the receiver and transmitter antenna results in a nonhorizontal scattering plane. The scattering plane is defined as the plane formed by the transmitter and receiver antenna points and the center point of the common volume. It is convenient to specify the orientations of the antennas related to the local horizontal plane. In general, the scattering plane will not be parallel to the horizontal plane. Therefore the horizontal and vertical orientation vectors of the transmitted signal related to the scattering plane must first be calculated. Following this, the bistatic scattering may be calculated and the resulting signal may be transformed into the local horizontal and vertical coordinate planes of the receiver antenna. It is vital that the impact of link geometry on the bistatic coupling be taken into account as it has in the analysis presented here.

2.4. Attenuation

Gaseous attenuation due to oxygen and attenuation due to rain are the dominant contributors to excess attenuation on the link path from the transmitter to the receiver. Water vapor attenuation is negligible by comparison.

The oxygen molecule has a permanent magnetic moment which gives rise to frequency-dependent absorption of incident electromagnetic energy. When an electromagnetic wave impinges on an oxygen molecule, electrons transit within a single electron state. This interaction happens only at the resonant frequencies of the electrons. Between 58 and 66 GHz

there are 16 resonant frequencies, which results in significant oxygen attenuation centered around 60 GHz. For standard atmospheric conditions at sea level this is typically between 12 and 16 dB km⁻¹.

In 1985, Liebe proposed the microwave propagation model (MPM) to describe oxygen attenuation. This model has been well tested and is often used for modeling the gaseous attenuation, especially when the 60 GHz band is included in the frequency range. Further detailed discussion on the microwave propagation model can be found in [9–11].

The path attenuation due to rain is determined from ITU-R recommendation P.838-2 [12].

2.5. Drop size distribution

Many models have been proposed for raindrop size distribution. However, because of the high degree of variability of drop size distribution with time and location, finding a model that accurately represents observations is fraught with difficulty. In the absence of other data, the distribution that fitted best to the observed data was the Marshall-Palmer distribution. Uncertainty in the drop size distribution is one of the largest sources of errors in the bistatic scattering model.

3. VALIDATION OF THE MODEL

During the development of the model, results were regularly checked with other programs. The scattering calculations were checked with the program MiePlot [13]. Although it was designed for light scattering, the Mie theory is valid for all frequencies and therefore the model could be compared with this program. A good agreement between the model and the results of MiePlot was found.

4. MODEL VERSUS MEASUREMENTS

As part of an Ofcom study, rain scattering measurements at 60 GHz were made by QinetiQ [5, 6]. For the measurements, an experimental propagation link was established using a wideband channel-sounder. The transmitter antenna was fed with an RF power of +5.1 dBm. The transmitter and receiver antennas were lens horn antennas with a gain of 34.5 dBi. The beamwidth of the antennas was 3° which is comparable with that of typical commercial equipment. The receiver noise bandwidth was 120 MHz. The antennas were located in two buildings at QinetiQ's Great Malvern site, with a line-of-sight distance of 75 m.

For a 45° scattering angle, Figure 1 shows the measured received power, together with the calculated power (derived from the theoretical model) and the associated rainfall rate. It can be seen that there is good agreement between the calculated power and the measured data. Note that even the modest rainfall rates of this event can cause significant bistatic coupling.

Similar good agreement between the model and measurements was observed for several other events confirming the validity of the model.

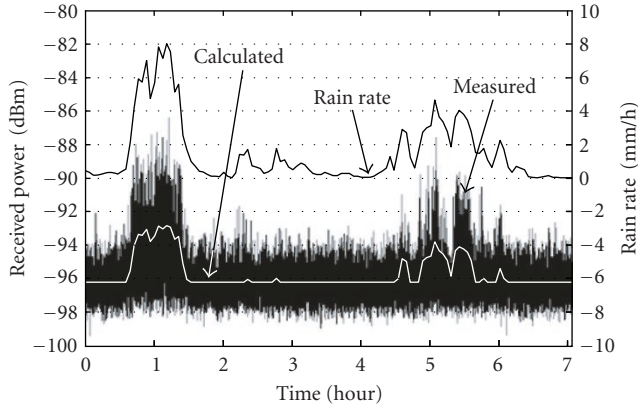


FIGURE 1: Received and calculated scattered power versus the rain rate.

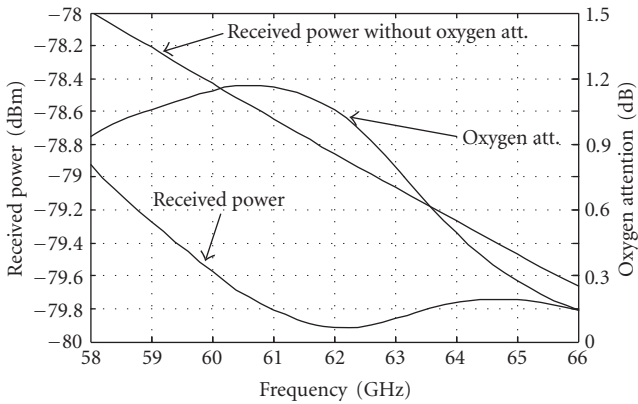


FIGURE 2: Influence of the frequency on received power.

5. MODELING 60 GHZ SCATTERING

Using the model, several scenarios were investigated to study the behavior of rain-induced bistatic scattering at 60 GHz. This analysis was performed to determine the general behavior in the case of link configurations not experimentally measured. This analysis highlighted some interesting results.

5.1. Influence of frequency

For the same link geometry as that of Figure 1, the frequency dependence from 58 GHz to 66 GHz was investigated. From Figure 2 it can be seen that the received power without taking the oxygen attenuation into account shows a linear decrease for increasing frequency. However, taking into account the significant oxygen attenuation changes this behavior. The large peak in the oxygen attenuation around 61 GHz changes the trend of the received power for frequencies above 62 GHz.

5.2. Scattering angle

The scattering angle can be formed by many different combinations of the antenna orientations, with two extremes: the

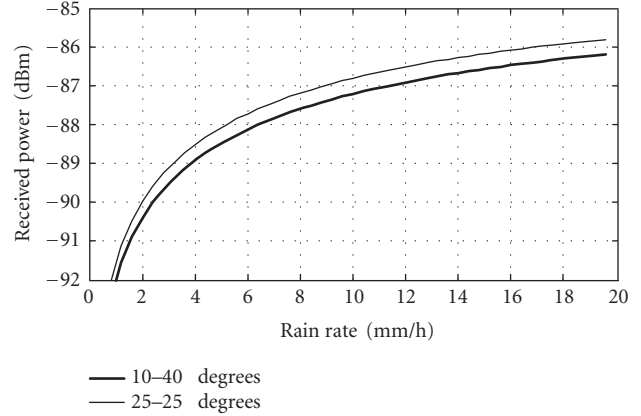


FIGURE 3: Received power versus rain rate for the same system settings and a different path orientation.

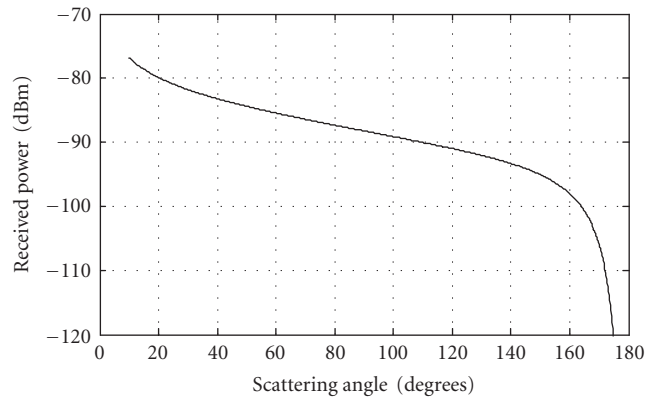


FIGURE 4: Received power versus scattering angle.

orientation of the transmitter and receiver antennas is the same (e.g., 40-40 degrees) or the orientation of one of the antennas is minimal and the other maximal (e.g., 10-70 degrees). The path length in case of the same orientation angle is larger than when the antenna orientations are maximally different. This results in a lower received scattered power. But the common volume for the same-orientation case is larger, resulting in more received scattered power. From the model simulations it appears that both effects almost cancel each other. The largest difference noticed is 0.5 dB in received power (see Figure 3), which is minimal.

The influence of the scattering angle on the received power was further investigated. Therefore an angular sweep of the scattering angle from 20 to 180 degrees was performed. This result is shown in Figure 4. This result is as one would intuitively expect; strong forward scattering and very weak backward scattering. This behavior has also been found at 94 GHz [4], therefore it confirms the model behavior.

6. CONCLUSION

A theoretical model for the calculation of bistatic scattering at 60 GHz has been presented. The theoretical model shows

good agreement with experimental data. It demonstrates that the first-order multiple scattering is sufficient to describe bistatic scattering by rain at 60 GHz. Using Mie theory for individual scattering by water spheres, we show that the bistatic scattered power reaches a maximum, which depends on the value of the scattering angle, the line-of-sight distance, and the frequency.

The modeling of the measured rain events shows that the model can predict the received scattered power for any configuration of interfering link. It is shown that the path orientation does not affect the received power very much, for constant system settings. The scattering angle does affect the received power very much, but the behavior it shows was expected, and confirms the model behavior.

This model shows good agreement between measured and calculated received powers. This shows that there is a relationship between scattered power and the rain rate, which can also be predicted, provided by the drop size distribution.

In the context of the wide deployment of 60 GHz links, it should be noted that coupling between adjacent links caused by bistatic scattering could be significant even in light rain ($<3 \text{ mm h}^{-1}$). This occurs in spite of the high oxygen attenuation. The effects of variable raindrop size distribution can also be significant. Although best agreement between model and measurements was found using a Marshall-Palmer raindrop size distribution, it should be noted that in many cases the Marshall-Palmer distribution can substantially overestimate the number of smaller raindrops, and therefore overestimate the scattered power. The use of the Marshall-Palmer distribution does however provide a “worst case” estimate that may be useful when considering high-availability links.

ACKNOWLEDGMENTS

We thank D. Eden of Ofcom and A. Shukla of QinetiQ for making available the experimental data used in this study. The data were collected under Ofcom Contract AY4497.

REFERENCES

- [1] A. Ishimaru, *Wave Propagation and Scattering in Random Media*, IEEE Press and Oxford University Press, New York, NY, USA, 1997.
- [2] M. Kerker, *The Scattering of Light and Other Electromagnetic Radiation*, Academic Press, London, UK, 1969.
- [3] R. K. Crane, “Bistatic scatter from rain,” *IEEE Transactions on Antennas and Propagation*, vol. 22, no. 2, pp. 312–320, 1974.
- [4] C. Gloaguen and L. Lavergnat, “94 GHz bistatic scattering in rain,” *IEEE Transactions on Antennas and Propagation*, vol. 44, no. 9, pp. 1247–1258, 1996.
- [5] R. M. Swindell and D. J. Fraser, “Improving spectrum utilisation at 58-66GHz through an accurate assessment of rain scatter interference phase 1 report,” QinetiQ/03/00084, 2003, unpublished.
- [6] R. M. Swindell, D. J. Fraser, and R. J. Watson, “Improving spectrum utilization at 58-66 GHz through an accurate assessment of rain scatter interference phase 2 report,” AY4487, QinetiQ, 2004, unpublished.
- [7] T. Oguchi, “Electromagnetic wave propagation and scattering in rain and other hydrometers,” *Proceedings of the IEEE*, vol. 71, no. 9, pp. 1029–1078, 1983.
- [8] H. C. van de Hulst, *Light Scattering by Small Particles*, Dover, New York, NY, USA, 1981.
- [9] H. J. Liebe, “MPM—an atmospheric millimeter-wave propagation model,” *International Journal of Infrared and Millimeter Waves*, vol. 10, no. 6, pp. 631–650, 1989.
- [10] A. C. Valdez, “Analysis of atmospheric effects due to atmospheric oxygen on a wideband digital signal in the 60 GHz band,” M.S. thesis, Department of Electrical Engineering, Virginia Polytechnic Institute and State University, Blacksburg, Va, USA, 2001.
- [11] G. Brussaard and P. A. Watson, *Atmospheric Modelling and Millimetre Wave Propagation*, Chapman & Hall, London, UK, 1995.
- [12] “Specific Attenuation Model for Rain for Use in Prediction Methods,” ITU-R, Recommendation P.838-2, 2003.
- [13] P. Laven, “MiePlot a computer program for scattering of light from a sphere using Mie theory & the Debye series,” January 2006, <http://www.philiplaven.com/mieplot.htm>.